

EFFECT OF HEAT TREATMENT ON THE ABRASIVE WEAR OF WELDED JOINTS OF MARTENSITIC STEEL WITH BORON

*M. Zemlik^{*1}, Ł. Konat*, B. Bialobrzeska*, K. Jamrozak***

** Department of Vehicle Engineering, Faculty of Mechanical Engineering,
Wrocław University of Science and Technology, Poland*

*** Department of Mechanics, Materials Engineering and Biomedical Engineering,
Faculty of Mechanical Engineering, Wrocław University of Science and Technology, Poland*

Abstract: The welding of martensitic steels in any case results in a reduction of mechanical properties and thus resistance to abrasive wear, both in the zone of the weld material and the broad heat-affected zone. This is due to the maximum strength of commercially available welding consumables not exceeding the tensile strength R_m value of 1000 MPa, which for steels with a claimed hardness of 500 HBW and a strength of min. 1500 MPa, results in a reduction of mechanical properties in the zone of the weld material by a minimum of 40% compared to the base material. To address this issue, the authors decided to subject welded joints of selected high-strength steel to comprehensive heat treatment procedures aimed at restoring the martensitic microstructure in the weld zone. The study demonstrated that the hardness of the weld material could be increased from 213 HBW in the as-welded state to 357 HBW after heat treatment. This improvement led to a corresponding increase in the relative abrasive wear resistance coefficient k_b , rising from 0.87 to 0.97, bringing it closer to that of the base material ($k_b = 1.00$).

Keywords: abrasive wear, martensitic steel, heat treatment, welding.

1. INTRODUCTION

Due to the fact that components working in the exploitation of deposits or working the soil, such as blades, coulters, excavator buckets, dippers, chutes or conveyor belts are exposed to direct contact with abrasive particles, numerous studies have focused on developing materials with maximized hardness [1]. In this case, the goal is to maintain a minimum hardness ratio of 1:1 between the abraded material and the abrasive [2]. Among the metallic materials used for such components there are Hadfield steel, materials containing carbide precipitations (hardfaced layers, alloyed cast iron, sintered carbides) and low-alloy, martensitic steels with boron. The advantage of the last-mentioned material group over the others is - declared by manufacturers - weldability.

Examples of these steels are Hardox, Raex, Perdur, Miilux, Brinar, and their designations are ranked according to hardness measured in 50 Brinell scale unit increments. The lowest grades typically exhibit a hardness of about 400 HBW, which corresponds to a tensile strength (R_m) of approximately 1286 MPa [3]. However, after welding tests, unfavorable changes are observed, which affect the significant shortening of the life of components made of the above materials. The formation of differentiated structures in all characteristic zones of the joint, as well as, in many cases, inadequately carried out heat treatment, abruptly reduce the resistance to abrasive wear of the discussed group of steels and lead to a dramatic reduction in their mechanical properties [4], [5], [6]. For example, knife strips made of Hardox 400 steel, mounted by welding techniques on the bucket, underwent wear in twice the time of those made of 18G2A (P355) steel, but the most intensive wear occurred not in the area of the base material, but in the broad heat-affected zone and weld material [3]. Tensile strength of commercially available welding consumables does not exceed 1000 MPa [7], which, for example, in the case of Hadox Extreme steel (average tensile strength $R_m = 2411$) [8], results in a decrease in mechanical properties in the zone of the weld material by a minimum of 60% compared to the base material.

¹ Author for contacts: PhD Eng. Martyna Zemlik
E-mail: martyna.zemlik@pwr.edu.pl

Starting from the generally accepted premise that high mechanical strength is crucial for resistance to abrasive wear [9], [10], it becomes evident that the microstructural changes induced by welding lead to a sharp reduction in all functional properties [11], [12], [13], [14]. This issue has been widely addressed in numerous studies [15], [16], [17], showing that the mechanical strength of welded joints can be significantly improved only through the use of advanced welding techniques or appropriately selected post-weld heat treatments [18], [19], [20]. Therefore, the purpose of this study is to thoroughly analyze the potential for welding low-alloy martensitic steels with boron, aiming to achieve wear resistance in the weld material zone and heat-affected zone comparable to that of the base material.

2. MATERIALS AND METHODS

Commercially available plates of martensitic steel (4 mm thick) with a declared hardness of 500 HBW was selected for the study. Analyses of chemical composition were performed by spectral method using a Leco GDS500A glow discharge emission analyzer (LECO Corporation, St. Joseph, MI, USA). During the analysis, the following parameters were used to allow ionization of the inert gas: $U = 1250$ V; $I = 45$ mA; 99.999% argon. The results obtained were the arithmetic average of at least five measurements. Based on the recorded values, it can be concluded that the analyzed material belongs to the group of medium-carbon low-alloy steels ($C = 0.26\%$), in which the use of boron micro-additions is characteristic — as even a content of 0.0008% leads to a pronounced increase in hardenability [21], [22] (Table 1 and 2). Moreover, the CEV value of 0.51 classifies it as a steel with fair weldability.

Table 1. Chemical composition and carbon equivalents of the analyzed steel. # – plate thickness, CEV – carbon equivalent according to IIW, CET – carbon equivalent according to SS-EN 1011-2.

| C | Mn | Cr | Ni | Mo | V | Cu | CEV | CET | # |
|--|------|------|------|-------|--------|-------|------|------|------|
| chemical element [wt %] | | | | | | | [%] | | [mm] |
| 0.26 | 1.23 | 0.21 | 0.04 | 0.003 | 0.0110 | 0.004 | 0.51 | 0.40 | 4 |
| CEV=C+Mn/6+(Cr+Mo+V)/5+(Cu+Ni)/15; CET=C+(Mn+Mo)/10+(Cr+Cu)/20+Ni/40 | | | | | | | | | |

Table 2. Chemical composition of the analyzed steel. # – plate thickness.

| Si | P | S | Al | Ti | Nb | Co | B | # |
|-------------------------|-------|-------|-------|-------|-------|--------|--------|------|
| chemical element [wt %] | | | | | | | | [mm] |
| 0.23 | 0.011 | 0.001 | 0.036 | 0.036 | 0.002 | 0.0050 | 0.0006 | 4 |

Welded joints were made by means of the MAG (metal active gas) method, using welding consumables dedicated to low-alloy high-strength steels (Table 3). The process was carried out using an ESAB A2 Mini Trac welding machine with an ESAB LAE 800 current source. The plates were joined by a double-sided weld, according to the following parameters to guarantee proper depth of fusion of the plates: weld type: BW (butt); welding position: PA (bottom-up); electrode diameter: 1.0 mm; arc voltage (1/2 weld): 15V/28.2V; current intensity (1/2 weld): 90A/170A; polarity: DC (+); wire feed speed: 9m/min; electrode wire: OK AristoRod89 (Mn4Ni2CrMo according to PN-EN ISO 16834-A); preheating: none; interlayer temperature: ≤ 80 °C; welding edge preparation (bevel): none.

A diagram of the completed welded joint is shown in Figure 1.

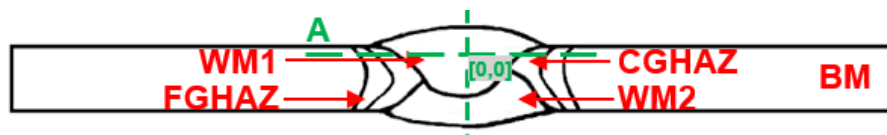


Figure 1. General schematic of the welded joints of analyzed martensitic steel. WM1/WM2 – individual weld material layers in the order they were made, BM – base material, CGHAZ/FGHAZ – coarse/fine-grained heat-affected zone, A – line of hardness distribution measurements.

Welding procedures were carried out using OK AristoRod™ 89 welding wire (Table 3). This is a solid wire without copper coating, designed for MAG welding of very high strength steel (yield strength R_p

< 900 MPa). OK AristoRod™ 89 is used for welding mainly in structures such as crane equipment, working machinery, trucks, cargo handling equipment, containers.

Table 3. Properties of the filler used to create the welded joint [23].

| Filler material | C | Mn | Si | Cr | Ni | Mo | R _{p0.2} | R _m | A | KV ₋₄₀ |
|------------------|-----------------------------|------|------|------|------|------|-------------------|----------------|-----|-------------------|
| | chemical composition [wt %] | | | | | | [MPa] | | [%] | [J] |
| OK AristoRod™ 89 | 0.10 | 1.90 | 0.80 | 0.30 | 2.10 | 0.65 | 920 | 960 | 18 | 55 |

The heat treatment procedures were carried out in Czylok's FCF 12SHM/R gas-tight chamber furnaces (FCF 12SHM/R by Czylok, Jastrzębie-Zdrój, Poland) using a protective atmosphere of 99.95% argon inert gas. The quenching bath was demineralized water at a temperature not exceeding 30 °C. Heat treatment was carried out according to the following parameters: double normalizing: 900°C, 2×30 min/air, quenching: 900°C, 20 min/water, tempering: 100°C, 5h. Normalization procedures were performed twice due to the significant amount of supplied heat input during manual MAG welding, which increased the prior austenite grain size. A single annealing step was insufficient to eliminate undesirable microstructural changes, which caused necessity of a second normalization. Hardness measurements were carried out using a Zwick/Roel ZHU 187.5 universal hardness tester (Zwick Roell Gruppe, Ulm, Germany) by the Brinell method, in accordance with PN-EN ISO 6506-1:2014-12. A carbide ball with a diameter of 2.5 mm was used, under a load of 187.5 kgf (1838.7469 N) applied for 15 seconds. Hardness measurements on cross-sections of welded joints were performed by the Rockwell method (HRA) in accordance with PN-EN ISO 6508-1:2016-10, using the above universal hardness tester, with a load of 60 kgf (588.399 N). The hardness results obtained were converted to Vickers scale in accordance with PN-EN ISO 18265:2014-02. The hardness measurements were carried out on cross sections of the specimens in the as-welded state and after heat treatment procedures. The locations of performed hardness distributions are schematically marked with line A in Figure 1.

A Nikon Eclipse MA200 light microscope (LM) was used for microscopic examination (Nikon Corporation, Tokyo, Japan). Samples were tested after etching with a 3% HNO₃ solution and Adler's reagent, according to PN-H-04503:1961. Nikon DS-Fi2 digital cameras coupled to the microscopes and Nikon NIS Elements software were used to record and analyze the recorded images.

Photographs of surfaces subjected to wear tests were taken with a Phenom XL scanning electron microscope (Eindhoven, The Netherlands), secondary electrons (SE) imaging and an accelerating voltage of 15 keV.

Abrasion resistance tests were performed using a T-07 tester (Radom, Poland) with loose abrasive, in accordance with the requirements of the ASTM G65 standard, under a constant load of $F = 44 \text{ N}$ ($\Delta F = 0.25 \text{ N}$). All heat treatment states were tested in six repetitions. The T-07 tribotester consisted of a rubber-rimmed steel wheel of diameter $\varnothing = 50 (+0.2) \text{ mm}$ and width $15 (-0.1) \text{ mm}$, an abrasive reservoir allowing for the regulation of abrasive flow, and a lever with weights generating a vertical pressing force of the sample against the roller. The hardness of the rubber applied to the roller was in the range of 78-85 ShA. For the tests, samples with dimensions of $30 \times 30 \times 10 \text{ mm}$ were prepared. Electrofused alumina No. 90 was used as the abrasive, according to ISO 8486-2:1998. The test duration was selected based on the hardness of the material and was 1800 roller revolutions (30 min.). Mass loss was measured on a laboratory balance with an accuracy of 0.0001 g. The aim of the study was to determine the relative abrasion resistance coefficient k_b concerning a reference sample, which was the base material. This abrasion resistance coefficient was defined according to the following formula (1):

$$k_b = \frac{Z_w \cdot \rho_b \cdot N_b}{Z_b \cdot \rho_w \cdot N_w} \quad (1)$$

where:

k_b – relative abrasion resistance coefficient, Z_w/Z_b – weight loss of reference samples/tested material in [g], N_w/N_b – number of roller revolutions during testing of the reference/tested sample, ρ_w, ρ_b – density of the reference sample material and the tested material [g/cm³].

3. RESULTS AND DISCUSSION

3.1. Metallographic analysis and hardness measurements

The parameters of the heat treatment applied to the welded joints were selected on the basis of the actual chemical composition, determined after the welding processes, both in the base material (Tables 1–2) and in the weld material zone (Table 4). The carbon content of the analyzed material of the tested welded joint is 0.16%. In addition, the material contains relatively high amounts of nickel (1.53%) and molybdenum (0.41%), as well as a boron micro-addition (0.0019%), all of which significantly enhance its hardenability. The above composition justifies the selection of the heat treatment temperature in the range of 880 – 900 °C.

Table 4. Chemical composition of the weld material.

| C | Mn | Si | P | S | Cr | Ni | Mo | V | Cu | Al | Ti | Nb | B |
|--------------------------|------|------|-------|-------|------|------|------|-------|------|-------|-------|-------|--------|
| chemical element [wt. %] | | | | | | | | | | | | | |
| 0.16 | 1.11 | 0.53 | 0.010 | 0.003 | 0.31 | 1.53 | 0.41 | 0.008 | 0.05 | 0.007 | 0.012 | 0.006 | 0.0019 |

The base material of the analyzed steel has an average hardness of 490 HV (Figure 2). The performance of welding processes results in a decrease in hardness in the zone of the weld material to 224 HV, which equals 45% of the value of the base material, while the low value obtained in the region of the heat-affected zone (217 HV) indicates the low hardenability of the steel. Carrying out normalizing before quenching is justified in order to refine the microstructure, and in this case, a value equal to nearly 250 HV is recorded for the weld material, while in the base material – despite the higher carbon content – it is 175 HV. The realization of complex heat treatment procedures raises the mechanical properties to 375 HV in the zone of the weld material – a value equal to approximately 77% of the base material.

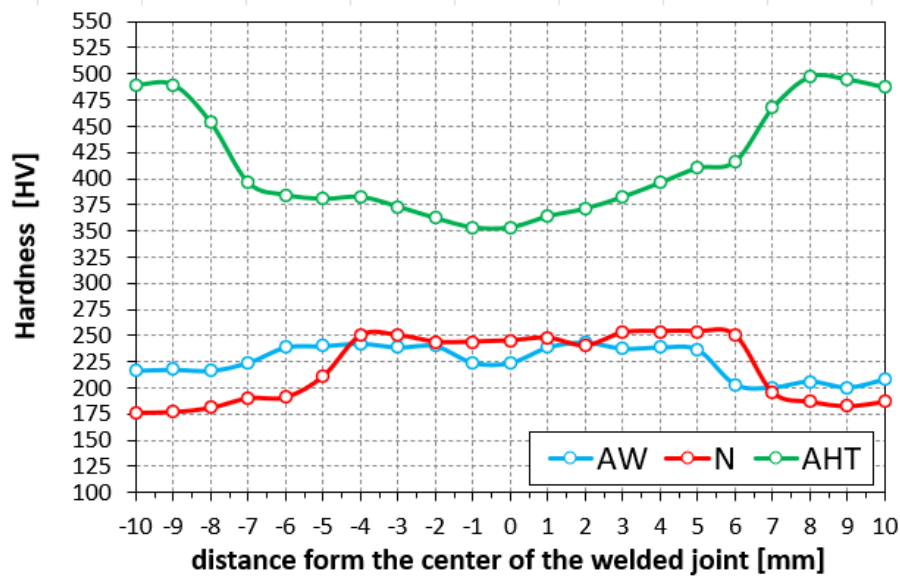


Figure 2. Hardness distribution of the analyzed welded joint along line A marked in Fig. 1, AW – joint after welding, AHT – heat-treated, N – as-normalized.

The microstructure of the analyzed steel consists of fine-tempered martensite with areas of quenched martensite (Fig. 3). Welding induces several microstructural changes. In the weld metal zone, a microstructure composed of acicular ferrite is observed (Fig. 4). The coarse-grained heat-affected zone (CGHAZ) consists of fine-dispersed pearlite and ferrite, with the banding being indistinct. These microstructures are consistent with hardness test results, which show a decrease from 490 HV in the base material to 217-224 HV in the analyzed zones. Comprehensive heat treatment results in

a uniform martensitic microstructure across all characteristic zones of the welded joint (Fig. 5). Due to the lower carbon content, the weld metal zone also contains a larger amount of quenched (fresh) martensite.

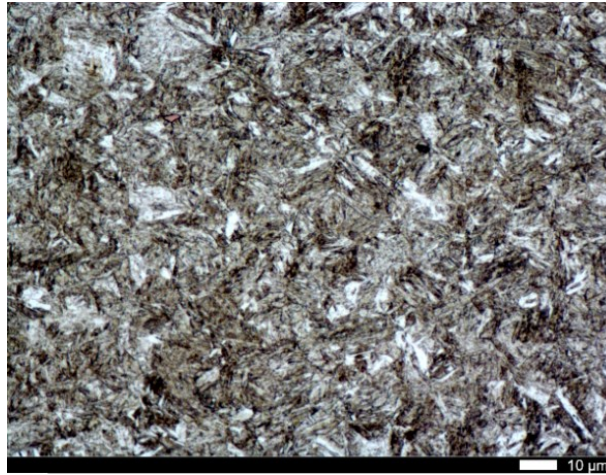


Figure 3. Microstructure of the analyzed steel. Light microscopy, etched with 3% HNO_3

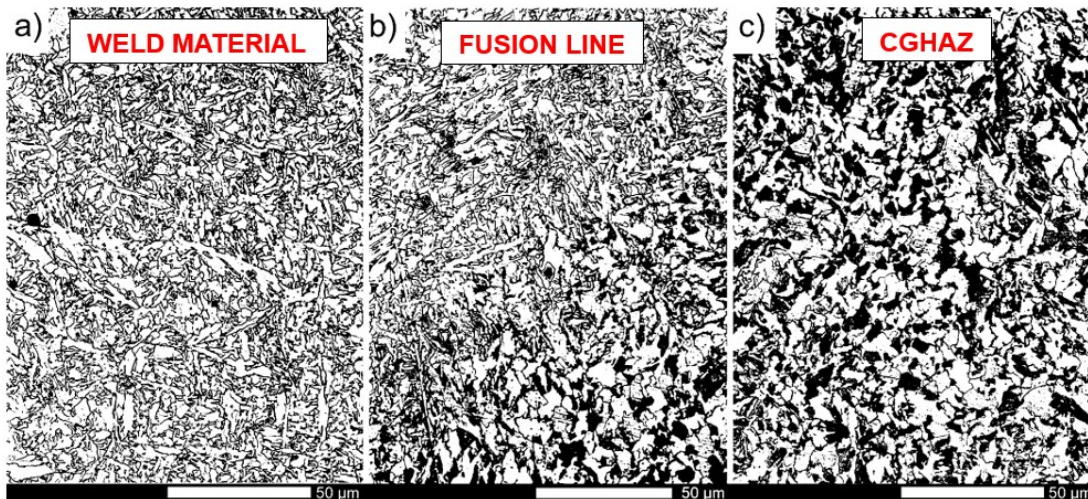


Figure 4. Microstructure of the analyzed as-welded welded joint. CGHAZ – coarse-grained heat-affected zone. Light microscopy, etched with 3% HNO_3 .

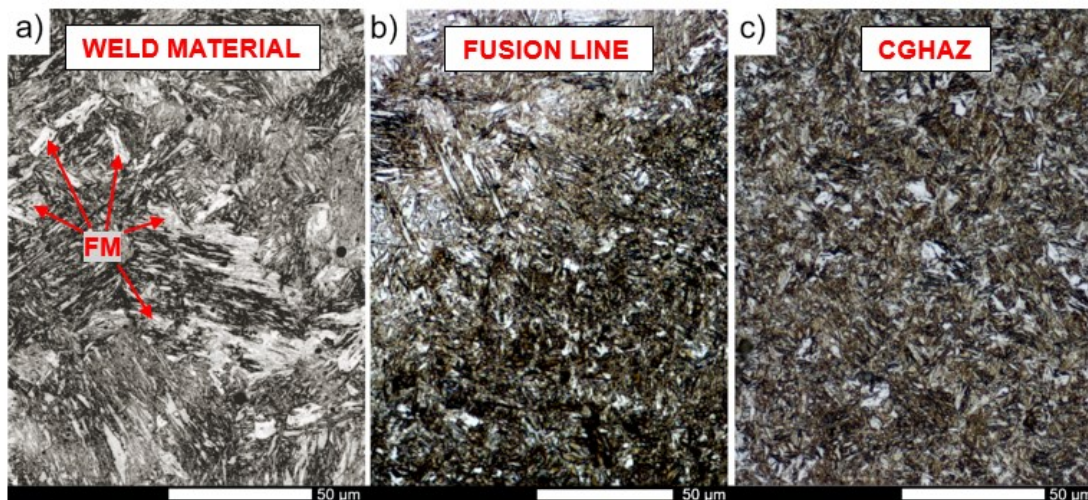


Figure 5. Microstructure of the analyzed welded joint after complex heat treatment. CGHAZ – coarse-grained heat-affected zone. FM – fresh martensite. Light microscopy, etched with 3% HNO_3 .

3.1. Abrasive wear resistance tests

The results of the abrasive wear tests are presented in Figure 6. According to the data, the highest relative abrasion resistance coefficient k_b was recorded for the base material (reference material, $k_b = 1.00 \pm 0.02$). Welding the steel leads to a decrease in the k_b value to 0.87 ± 0.02 in the weld material zone. However, after comprehensive heat treatment, the k_b value in this zone increases to 0.97 ± 0.01 . It is important to note that the difference in hardness between the base material and the welded joint is approximately 110 Brinell units, which translates into only a minor difference in the obtained wear indices. Additionally, a scatter greater than 0.03 is observed in steels of similar hardness in the as-delivered state, such as Hardox 500 and Brinar 500 (with k_b values of 1.20 and 1.11, respectively) [24] or 38 GSA steel (commercially used in Poland for ploughshares, hardness 555 HBW) and boron steel TBL PLUS (hardness 520 HBW) where the k_b values are equal to 1.25 and 1.29, respectively [25].

Literature suggests that these differences are influenced by the degree of solid solution strengthening [26], [27], [28], which affects the material's plastic properties and its ability to undergo work hardening under the pressure of abrasive particles. Considering the obtained values and the differences in chemical composition between the base material and the weld material, it appears reasonable to use a nickel additive while reducing the carbon content. Similar relationships were also observed in the study [10], where Hardox 600 steel, despite its lower hardness, demonstrated less mass loss compared to Hardox Extreme. Another example includes steels with a complex bainitic-martensitic microstructure containing retained austenite and finely dispersed carbides, achieved through tailored chemical composition and controlled slow cooling after quenching. In such cases, steels with a hardness of 470 HBW have shown wear coefficient k_b comparable to those of 600 HBW grades [25]. As in the findings presented in this paper, tribological performance in these examples has been linked to structural deformation.

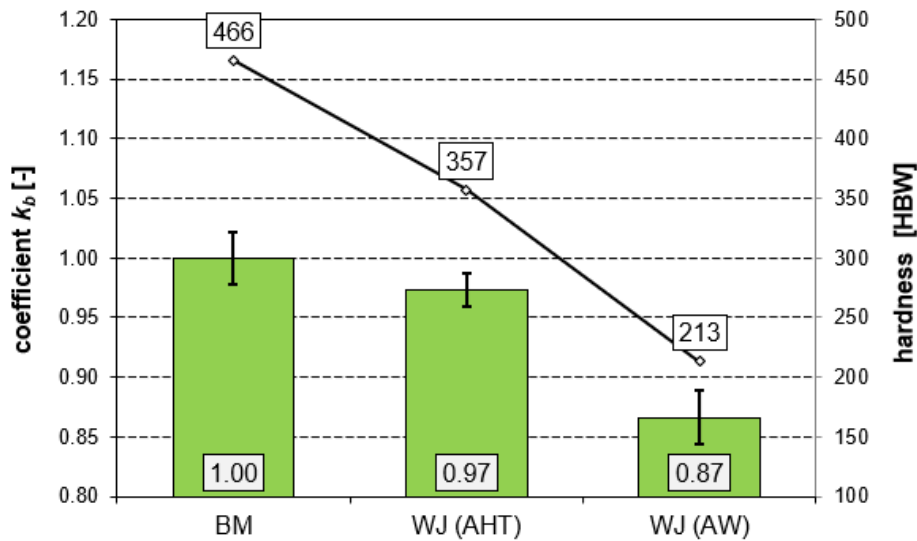


Figure 6. Relative abrasion resistance coefficient k_b : WJ (AW) - welded joint in the as-welded condition, WJ (AHT) - welded joint after heat treatment.

The above observations were reflected in the microstructure of the surface after the wear tests. In the case of the base material, the dominant wear mechanisms are microploughing, microcutting and scratching (chips formation). Material loss occurs mainly through the detachment of surface fragments (pits), which precedes the onset of plastic deformation. In the case of as-welded joint, significant material loss and wear marks by microploughing are mainly observed. After comprehensive heat treatment procedures, the presence of wide plastic deformation on the analyzed surface should be indicated. Moreover, the resulting pits are narrow, and the material is worn mainly by microploughing and scratching. Such a condition justifies similar wear rates compared to the base material, where an additional wear mechanism is microcutting, resulting, unlike microploughing, in a mass loss.

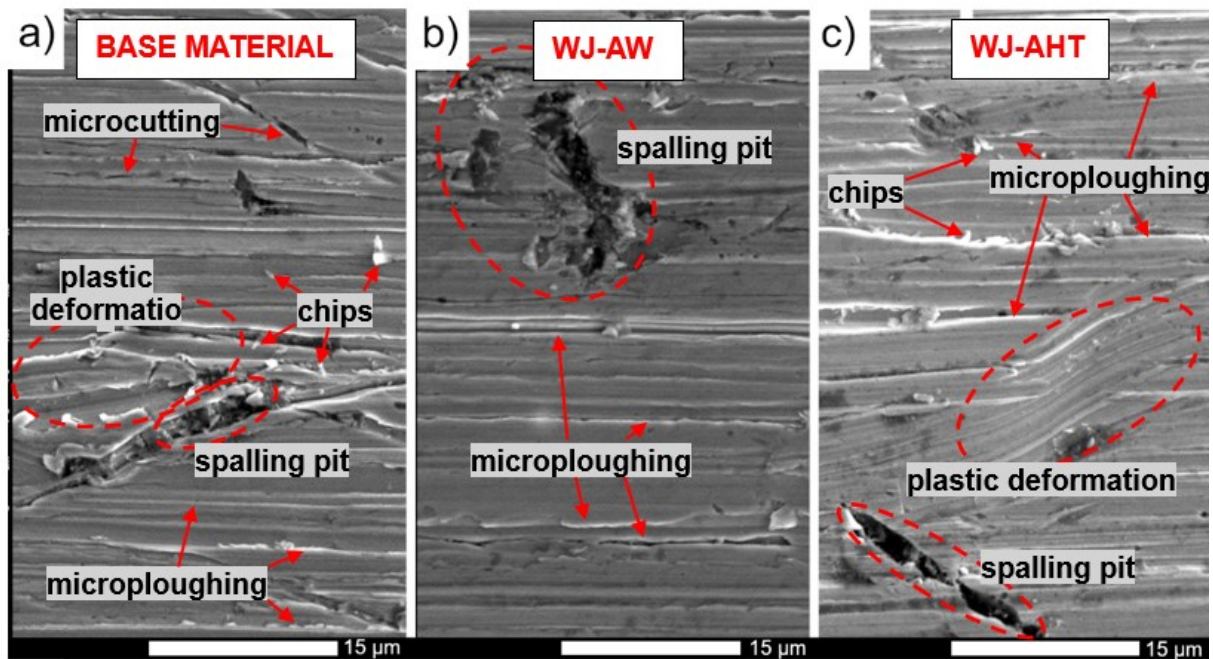


Figure 7. Images of the worn surfaces subjected to testing with the use of T-07 device. WJ (AW) - welded joint in the as-welded condition, WJ (AHT) - welded joint after heat treatment. SEM, unetched.

4. CONCLUSIONS

Based on the presented study, the following conclusions can be drawn:

- The analyzed steel exhibits a hardness of 490 HV (466 HBW). After heat treatments, the hardness in the weld material zone decreases to 224 HV (213 HBW), which is approximately 45% of the base material's hardness. However, comprehensive heat treatments increase the hardness in the weld zone to 375 HV (357 HBW), reaching approximately 77% of the base material's hardness.
- Welding of the martensitic steel results in significant microstructural changes in both the weld material zone and the heat-affected zone. In the weld material zone, a microstructure of needle-like ferrite is observed, while the coarse-grained heat-affected zone exhibits a complex structure composed of ferrite and finely dispersed pearlite.
- Welding treatments reduce the relative abrasion resistance coefficient k_b to 0.87 ± 0.02 in the weld material zone, compared to the base material (reference material, $k_b = 1.00 \pm 0.02$). Comprehensive heat treatments improve the k_b value in the weld material zone to 0.97 ± 0.01 .
- In the base material, the predominant wear mechanisms are microploughing, microcutting, and scratching (chip formation), with material loss occurring primarily through the detachment of surface fragments (pits). In the as-welded joint, significant material loss and wear marks due to microploughing are observed. After comprehensive heat treatment, extensive plastic deformation is noticeable on the surface. This condition explains the similar wear rates compared to the base material, where an additional wear mechanism, microcutting, causes greater weight loss compared to microploughing.

REFERENCES

- [1] B. Białobrzeska, "The influence of boron on the resistance to abrasion of quenched low-alloy steels," *Wear*, vol. 500–501, p. 204345, Jul. 2022, doi: 10.1016/j.wear.2022.204345.
- [2] K.-H. Z. Gahr, "Wear by hard particles," *Tribol Int*, vol. 31, no. 10, pp. 587–596, Oct. 1998, doi: 10.1016/S0301-679X(98)00079-6.
- [3] Ł. Konat and G. Pękalski, "Overview of Materials Testing of Brown-Coal Mining Machines (Years 1985–2017)," in *Mining Machines and Earth-Moving Equipment*, Cham: Springer International Publishing, 2020, pp. 21–58. doi: 10.1007/978-3-030-25478-0_2.
- [4] S. Baskutis *et al.*, "Influence of Additives on the Mechanical Characteristics of Hardox 450 Steel Welds," *Materials*, vol. 16, no. 16, p. 5593, Aug. 2023, doi: 10.3390/ma16165593.

- [5] T. Teker and D. Gençdoğan, "Mechanical performance and weldability of HARDOX 450/AISI 430 grade joined by TIG double-sided arc welding," *Materials Testing*, vol. 64, no. 11, pp. 1606–1613, Nov. 2022, doi: 10.1515/mt-2022-0090.
- [6] A. P. Silva, T. Węgrzyn, T. Szymczak, B. Szczucka-Lasota, and B. Łazarz, "Hardox 450 Weld in Microstructural and Mechanical Approaches after Welding at Micro-Jet Cooling," *Materials*, vol. 15, no. 20, p. 7118, Oct. 2022, doi: 10.3390/ma15207118.
- [7] ESAB, "Welding Consumables," 2012.
- [8] B. Białobrzeska, R. Jasiński, Ł. Konat, and Ł. Szczepański, "Analysis of the Properties of Hardox Extreme Steel and Possibilities of Its Applications in Machinery," *Metals (Basel)*, vol. 11, no. 1, p. 162, Jan. 2021, doi: 10.3390/met11010162.
- [9] M. Zemlik, Ł. Konat, and D. Grygier, "Influence of tempering temperature on the abrasive wear of high-strength, martensitic boron steel Hardox Extreme," *Tribologia*, vol. 303, no. 1, pp. 97–106, Mar. 2023, doi: 10.5604/01.3001.0016.2937.
- [10] K. Ligier, M. Zemlik, M. Lemecha, Ł. Konat, and J. Napiórkowski, "Analysis of Wear Properties of Hardox Steels in Different Soil Conditions," *Materials*, vol. 15, no. 21, p. 7622, Oct. 2022, doi: 10.3390/ma15217622.
- [11] T. Ślęzak and L. Śnieżek, "Fatigue Properties and Cracking of High Strength Steel S1100QL Welded Joints," *Key Eng Mater*, vol. 598, pp. 237–242, Jan. 2014, doi: 10.4028/www.scientific.net/KEM.598.237..
- [12] K. Ligier, M. Bramowicz, S. Kulesza, M. Lemecha, and B. Pszczółkowski, "Use of the Ball-Cratering Method to Assess the Wear Resistance of a Welded Joint of XAR400 Steel," *Materials*, vol. 16, no. 13, p. 4523, Jun. 2023, doi: 10.3390/ma16134523.
- [13] K. Ligier, J. Napiórkowski, and M. Lemecha, "Assessment of Changes in Abrasive Wear Resistance of a Welded Joint of Low-Alloy Martensitic Steel Using Microabrasion Test," *Materials*, vol. 17, no. 9, p. 2101, Apr. 2024, doi: 10.3390/ma17092101.
- [14] M. Zemlik, Ł. Konat, and B. Białobrzeska, "Analysis of the possibilities to increase abrasion resistance of welded joints of Hardox Extreme steel," *Tribol Int*, vol. in press, 2025, doi: 10.1016/j.triboint.2024.110271.
- [15] A. Lisiecki, A. Kurc-Lisiecka, W. Pakieła, G. Chrobak, G. F. Batalha, and M. Adamiak, "Laser Welding of ARMOX 500T Steel," *Materials*, vol. 17, no. 14, p. 3427, Jul. 2024, doi: 10.3390/ma17143427.
- [16] M. Kuciewicz, P. Prochenka, J. Janiszewski, and J. Małachowski, "Numerical-experimental analysis of laser-welded small energy absorbers with direct impact Hopkinson method," *J Constr Steel Res*, vol. 218, p. 108746, Jul. 2024, doi: 10.1016/j.jcsr.2024.108746.
- [17] G. Turichin *et al.*, "Laser-Arc hybrid welding perspective ultra-high strength steels: influence of the chemical composition of weld metal on microstructure and mechanical properties," *Procedia CIRP*, vol. 74, pp. 752–756, 2018, doi: 10.1016/j.procir.2018.08.017.
- [18] Ł. Konat, "Technological, Microstructural and Strength Aspects of Welding and Post-Weld Heat Treatment of Martensitic, Wear-Resistant Hardox 600 Steel," *Materials*, vol. 14, no. 16, p. 4541, Aug. 2021, doi: 10.3390/ma14164541.
- [19] Konat, "Structural Aspects of Execution and Thermal Treatment of Welded Joints of Hardox Extreme Steel," *Metals (Basel)*, vol. 9, no. 9, p. 915, Aug. 2019, doi: 10.3390/met9090915.
- [20] Ł. Konat, M. Zemlik, R. Jasiński, and D. Grygier, "Austenite Grain Growth Analysis in a Welded Joint of High-Strength Martensitic Abrasion-Resistant Steel Hardox 450," *Materials*, vol. 14, no. 11, p. 2850, May 2021, doi: 10.3390/ma14112850.
- [21] A. Deva, S. K. De, V. Kumar, M. Deepa, and B. K. Jha, "Influence of Boron on the Hardenability of Unalloyed and Low Alloyed Steel," *International Journal of Metallurgical Engineering*, vol. 2, no. 1, pp. 47–51, 2013, doi: 10.5923/j.ijmee.20130201.07.
- [22] B. Białobrzeska, "Effect of Alloying Additives and Microadditives on Hardenability Increase Caused by Action of Boron," *Metals (Basel)*, vol. 11, no. 4, p. 589, Apr. 2021, doi: 10.3390/met11040589.
- [23] ESAB, "Welding Consumables," 2012.
- [24] B. Białobrzeska and Ł. Konat, "Comparative analysis of abrasive-wear resistance of Brinar and Hardox steels," *Tribologia*, vol. 272, no. 2, pp. 7–16, 2017, doi: 10.5604/01.3001.0010.6261.
- [25] M. Zemlik, Ł. Konat, and J. Napiórkowski, "Comparative Analysis of the Influence of Chemical Composition and Microstructure on the Abrasive Wear of High-Strength Steels," *Materials*, vol. 15, no. 14, p. 5083, Jul. 2022, doi: 10.3390/ma15145083.
- [26] J. Mondal, K. Das, and S. Das, "An investigation of mechanical property and sliding wear behaviour of 400Hv grade martensitic steels," *Wear*, vol. 458–459, p. 203436, Oct. 2020, doi: 10.1016/j.wear.2020.203436.
- [27] N. Ojala *et al.*, "Effects of composition and microstructure on the abrasive wear performance of quenched wear resistant steels," *Wear*, vol. 317, no. 1–2, pp. 225–232, Sep. 2014, doi: 10.1016/j.wear.2014.06.003.
- [28] A. Jafari, K. Dehghani, K. Bahaaddini, and R. Abbasi Hataie, "Experimental comparison of abrasive and erosive wear characteristics of four wear-resistant steels," *Wear*, vol. 416–417, pp. 14–26, Dec. 2018, doi: 10.1016/j.wear.2018.09.010.